Technologies and Materials for Renewable Energy, Environment & Sustainability

Single-Mode Analytical Modeling of Geometrically Nonlinear Free Vibrations in Cable-Stayed Beams with Elastic Supports

AIPCP25-CF-TMREES2025-00039 | Article

Single-Mode Analytical Modeling of Geometrically Nonlinear Free Vibrations in Cable-Stayed Beams with Elastic Supports

Mohamed BERJAL[1, a)], Ahmed ADRI[1, b)], Issam EL HANTATI[2, c)], Omar OUTASSAFTE[1, d)], Yassine EL KHOUDDAR[3, e)], Mohamed RJILATTE[1, f)] and Rhali BENAMAR[4, g)]

[1,] *Laboratory of Process Engineering, Mechanics, Materials and Industrial Engineering (LP2MGI), High School of Technology (ESTC), Hassan II University, Casablanca, Morocco.*
[2] *Laboratory of Mechanical, Engineering and Innovation (LM2I), National Higher School for Electricity and Mechanics (ENSEM), Hassan II University, Casablanca, Morocco.*
[3] *Engineering of Complex Systems and Structures (ECSS), National Higher School of Arts and Crafts (ENSAM) Université Moulay Ismail, Meknes, Morocco.*
[4] *Simulation Studies and Research Laboratory, Instrumentation and Measurements (LERSIM), Mohammadia School of Engineers (EMI), Mohammed V University, Rabat, Morocco.*

[a)] *Corresponding author: mohamed.berjal.doc22@ensem.ac.ma*
[b)] *ahmedadri@gmail.com*
[c)] *hantati.issam@gmail.com*
[d)] *omar.outassafte@ensem.ac.ma*
[e)] *elkhouddar.yassine@gmail.com*
[f)] *mohamed.rjilatte.doc22@ensem.ac.ma*
[g)] *rhali.benamar@gmail.com*

Abstract. Cable-stayed beams are a fundamental research area in structural engineering due to their complex dynamic behavior and their widespread application in long-span structures, which motivates sustained research in both civil and mechanical engineering. The present study focuses on examining the geometric nonlinearity affecting the large-amplitude free vibrations of a beam supported by a symmetric cable system, adopting a single-mode analytical approach. General theoretical formulations are established for a multi-stayed beam based on Euler–Bernoulli beam theory, specifically integrating the nonlinear geometric effects induced by the cables' initial sag. A segmented model of the multi-cable beam is developed, and the resulting homogeneous system is solved numerically using the Newton–Raphson method to determine the natural frequencies and associated linear displacement fields. The analysis addresses the nonlinear problem by expanding the displacement function into a series based on the linear modes, which yields discrete expressions for the strain energy and kinetic energy. Under the influence of a point excitation, the nonlinear algebraic system derived from Hamilton's principle is solved via the application of the Benamar method. Ultimately, this investigation highlights the significant influence of geometric nonlinearity on the free vibrational behavior and quantifies the impact of key geometric parameters on the dynamic response of cable-suspended beams.

INTRODUCTION

Cable–beam systems, which combine flexible cables with elastic beams, offer significant advantages in civil and mechanical engineering, particularly for long-span structures. Their design improves efficiency and performance but leads to complex dynamic behavior due to large deformations and heavy loads, resulting in geometrically nonlinear vibrations. Despite growing academic interest, studies addressing these nonlinear dynamics remain limited.

Several recent works have contributed to this topic. Berjal and al. (2024) [1] investigated the influence of support stiffness on the natural frequencies of cable-stayed beams, while Rjilatte and al. (2024) [2] examined thermal effects and concentrated masses. Kang and al. (2022) [3] highlighted the hardening behavior caused by cable–deck coupling. Other studies, such as Peng and al. (2019) [4] and Gattulli & Lepidi (2003) [5], analyzed time-delay control and internal resonances, respectively. Azrar and al. (1999) [6] and El Kadiri & Benamar (2002) [7] proposed analytical formulations for nonlinear vibrations, followed by El Hantati and al. (2024) [8] and Outassafte and al. (2023) [9], who

extended the analysis to FGM beams and crack detection. Furthermore, Oudra et al. (2024) [10] conducted optimization and advanced-design studies aimed at improving the vibrational performance of intelligent FGM structures.

Building on these contributions, and following the previous works of El Hantati and al. (2022) [11] and El Khouddar and al. (2021) [12], the present research performs a parametric analysis of the geometrically nonlinear vibration behavior of a cable-stayed beam. The methodology relies on a linear modal analysis as the foundation for a nonlinear model, solved using the implicit Benamar method, recognized for its accuracy in studying complex vibrating structures.

METHOD

Linear Formulation

The present study develops a simplified structural model of a cable-stayed bridge deck, represented by a continuous beam supported by multiple inclined cables (Figure 1). The beam, simply supported at its ends, is equipped with translational and rotational elastic supports characterized by stiffness coefficients K_{ti} and $K_{\theta i}$. The beam–cable junctions divide the main girder into discrete segments, each treated as an independent beam element for structural analysis purposes.

The static equilibrium configuration is described through the cable displacements u_{cj}, v_{cj}, w_{cj} and the transverse displacements of the beam v_{bi}. Each cable is assumed to follow a parabolic profile given by $y_{cj} = 4d_{cj}[x_{cj}/l_{cj} - (x_{cj}/l_{cj})^2]$, where the sag-to-span ratio d_{cj}/l_{cj} remains below 1/10.

The pylons anchoring the cables are considered rigid, as experimental and finite-element studies indicate negligible vibration amplitudes. Due to the dominant axial stiffness of the beam ($E_bA_b/l_b >> 48E_bA_b/l_b^3$), axial deformations are disregarded. Furthermore, the horizontal component of cable tension has a minor influence on the overall response and is therefore neglected, following the assumptions established in Gattulli (2002) [13].

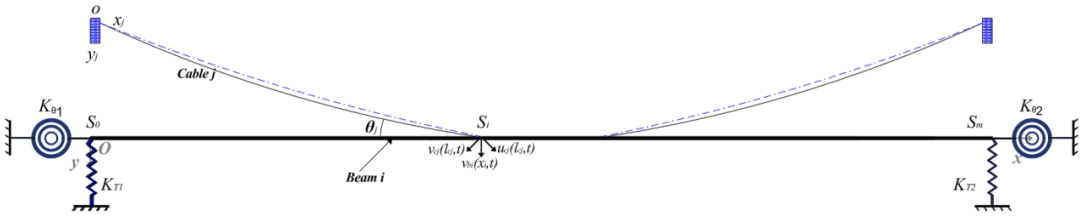

FIGURE 1. Configurations of multiple cable-stayed beams with multiple elastic supports

In accordance with the stated assumptions, Hamilton's variational principle is employed to derive the differential equations governing the coplanar motion, following an appropriate reduction of the structural model.

$$\begin{gathered} m_{bi}\frac{\partial^2 v_{bi}^*(x_i)}{\partial t^2} + \xi_{bi}^*\frac{\partial v_{bi}(x_i)}{\partial t} + E_{bi}I_{bi}v_{bi}^{iv^*}(x_i) = 0 \\ where\ \ s_{i-1} < x_i < s_i \\ m_{cj}\frac{\partial^2 v_{cj}^*}{\partial t^2} + \xi_{cj}^*\frac{\partial v^*{}_{cj}}{\partial t} - [H_{cj}\frac{\partial^2 v_{cj}^*}{\partial x_{cj}^2} + E_{cj}A_{cj}(\frac{\partial^2 y_j^*}{\partial x_{cj}^2} + \frac{\partial^2 v_{cj}^*}{\partial x_{cj}^2})e_j^*(t)] = 0 \end{gathered} \tag{1}$$

e_{cj} denotes the uniform dynamic elongation of cable j.

$$\begin{gathered} e_j{}^*(t) = \frac{u_{cj}^*(l_{cj},t)}{l_{cj}} + \frac{1}{l_{cj}}\int_0^{l_{cj}}\left(\frac{\partial y_j^*}{\partial x_j}\frac{\partial v_{cj}^*}{\partial x_j} + \frac{1}{2}\left(\frac{\partial v_{cj}^*}{\partial x_j}\right)^2\right)dx_j^* \\ (j = 1, 2, \dots, n;\ i = 1, 2, \dots, n+1) \end{gathered} \tag{2}$$

The analysis is based on the boundary conditions of the beam as previously discussed. The upper end of each cable is assumed to be rigidly fixed to the tower, while the lower end is anchored to the beam. Consequently, the composite

system must satisfy both the continuity requirements and the geometric boundary conditions described in Berjal and al. (2024) [14].

To achieve more general conclusions, dimensionless variables are introduced as detailed in [15]. This transformation allows the fundamental equations (1) and (2) to be reformulated in a non-dimensional form, ensuring their generality and independence from physical units. Such normalization enhances the physical interpretation of the results and facilitates comparative analysis with previous studies. Moreover, the boundary conditions are expressed in a dimensionless format, as specified in [15].

The model developed in this study corresponds to a symmetrically cable-stayed beam (double-cable configuration). Based on the theoretical framework previously established and under specific geometric conditions, namely cable anchorage points located at one-third of the span and an inclination angle of 30°, the following variable transformations are introduced to facilitate the subsequent formulation.

$$H_{cj} = H_c, d_j = d, \theta_j = \theta, m_{cj} = m_c, E_{cj}A_{cj} = E_cA_c,\ l_{cj} = l_c,\ \gamma_{cj} = \gamma_c, m_{bi} = m_b, E_{bi}I_{bi} = E_bI_b,\quad j = 1,2;\ i = 1,2,3 \tag{3}$$

The variable d_j represents the dimensionless deflection of the j th cable. Consequently, the application of the method of separation of variables allows establishing the following relationship:

$$\begin{aligned} v_{cj} &= w_{cj}(x)e^{i(\omega/\omega 0)\tau};(j = 1,2) \\ v_{bi} &= w_{bi}(x)e^{i(\omega/\omega 0)\tau};(i = 1,2,3) \end{aligned} \tag{4}$$

In addition, the corresponding boundary conditions are derived as follows, taking into account the elastic translational and rotational supports introduced at both ends of the beam.

$$\begin{aligned} &\left.\frac{\partial^3 w_{b1}}{\partial {x_i}^3}\right|_{x_i=0} = K_{T1}w_{b1}(0),\ \left.\frac{\partial^3 w_{b3}}{\partial {x_i}^3}\right|_{x_i=1} = -K_{T2}w_{b3}(1),\ \left.\frac{\partial^2 w_{b1}}{\partial {x_i}^2}\right|_{x_i=0} + K_{\theta 1}\left.\frac{\partial w_{b1}}{\partial x_i}\right|_{x_i=0} = 0, \\ &\left.\frac{\partial^2 w_{b3}}{\partial {x_i}^2}\right|_{x_i=1} - K_{\theta 2}\left.\frac{\partial w_{b3}}{\partial x_i}\right|_{x_i=1} = 0,\ w_{c2}(1) = \gamma_2 w_{b2}(s_2)\cos\theta, \\ &w_{b1}(0) = w_{b3}(1) = \left.\frac{\partial^2 w_{b1}}{\partial {x_i}^2}\right|_{x_i=0} = \left.\frac{\partial^2 w_{b3}}{\partial {x_i}^2}\right|_{x_i=1} = 0,\ w_{b1}(s_1) = w_{b2}(s_1), \left.\frac{\partial w_{b1}}{\partial x_i}\right|_{x_i=s_1} = \left.\frac{\partial w_{b3}}{\partial x_i}\right|_{x_i=s_2}, \\ &\left.\frac{\partial^2 w_{b1}}{\partial {x_i}^2}\right|_{x_1=s_1} = \left.\frac{\partial^2 w_{b2}}{\partial {x_i}^2}\right|_{x_i=s_2},\ w_{b2}(s_2) = w_{b3}(s_2), \left.\frac{\partial w_{b2}}{\partial x_i}\right|_{x_i=s_2} = \left.\frac{\partial w_{b3}}{\partial x_i}\right|_{x_i=s_2}, \left.\frac{\partial^2 w_{b2}}{\partial {x_i}^2}\right|_{x_1=s_2} = \left.\frac{\partial^2 w_{b3}}{\partial {x_i}^2}\right|_{x_i=s_2}, \\ &\chi\left[\left.\frac{\partial^3 w_{b1}}{\partial {x_i}^3}\right|_{x_i=s_1} - \left.\frac{\partial^3 w_{b2}}{\partial {x_i}^3}\right|_{x_i=s_1}\right] - \left(\sin\theta + \left.\frac{\partial y_1}{\partial x_i}\right|_{x_i=1}\cos\theta_1\right)\hat{e}_1 - \frac{\cos\theta}{\mu}\left.\frac{\partial w_{c1}}{\partial x_i}\right|_{x_i=1} = 0, \\ &\chi\left[\left.\frac{\partial^3 w_{b2}}{\partial {x_i}^3}\right|_{x_i=s_2} - \left.\frac{\partial^3 w_{b3}}{\partial {x_i}^3}\right|_{x_i=s_2}\right] - \left(\sin\theta + \left.\frac{\partial y_2}{\partial x_i}\right|_{x_i=1}\cos\theta_1\right)\hat{e}_2 - \frac{\cos\theta}{\mu}\left.\frac{\partial w_{c2}}{\partial x_i}\right|_{x_i=1} = 0, \end{aligned} \tag{5}$$

The analysis of the previously derived equations allows the solutions to be expressed in the following form:

$$\begin{aligned} w_{bi}(x) &= A_{ib}\cos\beta_b x + B_{ib}\sin\beta_b x + C_{ib}\cosh\beta_b x + D_{ib}\sinh\beta_b x \quad (i = 1,2,3) \\ w_{cj}(x) &= E_{jc}\sin\beta_c x + F_{jc}\cos\beta_c x + D_{jc} \quad (j = 1,2) \end{aligned} \tag{6}$$

Nonlinear Formulation

According to Hamilton's principle, the dynamic behavior of the system can be formulated as follows:

$$\delta\left(\int_0^{2\pi/\omega}(T - V)\,dt\right) = 0 \tag{7}$$

The kinetic energy of the beam is denoted by T, while V represents the total strain energy. The latter consists of two components: the bending strain energy, V_b, and the strain energy associated with the axial (normal) forces, V_a, which introduce the geometric nonlinearity of the system for each beam.

By introducing $\dot{W} = \frac{\partial W}{\partial t}$, which denotes the time derivative of the transverse displacement, the kinetic energy can be expressed as follows, in accordance with the formulation proposed in [16] :

$$T = \frac{1}{2}\rho_b S_b \int_0^{L_b} \left(\frac{\partial w_b(x,t)}{\partial t}\right)^2 dx \tag{8}$$

By introducing $W'' = \frac{d^2W}{dx^2}$, which represents the second derivative of the transverse displacement with respect to the longitudinal coordinate x, the bending strain energy V_b, together with the translational and rotational spring contributions $V_{T\ spring}$and $V_{R\ spring}$, can be expressed as follows:

$$V_b = \frac{E_b I_b}{2}\int_0^{L_b}\left(\frac{\partial^2 w_b(x,t)}{\partial x^2}\right)^2 dx + \frac{E_c A_c (sin\,\theta)^2}{2} w_b(x,t)\int_0^{L_c} w_b(x,t)dx \tag{9}$$

$$V_{T\ spring} = \frac{1}{2}\sum_{i=1}^{n} K_{T\ Sring}\left(w_b\left(x_{T\ Sring},t\right)\right)^2 \tag{10}$$

$$V_{R\ spring} = \frac{1}{2}\sum_{i=1}^{n} K_{R\ Sring}\left(\frac{\partial w_b(x_{R\ Sring},t)}{\partial x}\right)^2 \tag{11}$$

The strain energy associated with the axial (normal) forces, which are responsible for the geometric nonlinearity of the system, is denoted by V_a and can be expressed for each beam as follows:

$$\mathrm{V_a} = \frac{\mathrm{E_b I_b}}{8\mathrm{L}_b}\left[\int_0^b \left(\frac{\partial \mathrm{w}_b(\mathrm{x,t})}{\partial \mathrm{x}}\right)^2 \mathrm{dx}\right]^2 \tag{12}$$

In this analysis, the transverse displacement is expressed in terms of a modal expansion, constructed from a series of fundamental spatial functions $\phi_i(x)$, where i varies from 1 to N, with N representing the number of linear modes considered for the beam. These functions are associated with the generalized temporal coordinates $q_i(t)$, which are assumed to be harmonic in nature. Accordingly, the transverse displacement $W(x,t)$ can be written as follows:

$$\mathrm{w(x,t)} = \mathrm{a_i W(x)\sin(\omega t)} \tag{13}$$

By introducing the constant coefficients aia_iai into the previous energy expressions through Eq. (13), the following formulations are obtained:

$$\mathrm{V_b} = \frac{1}{2}\mathrm{a_i a_j k_{ij}}\sin^2(\omega \mathrm{t}) \tag{14}$$

$$\mathrm{V_a} = \frac{1}{4}\mathrm{a_i a_j a_k a_l b_{ijkl}}\sin^4(\omega \mathrm{t}) \tag{15}$$

$$\mathrm{T} = \frac{1}{2}\omega^2 \mathrm{a_i a_j m_{ij}}\cos^2(\omega \mathrm{t}) \tag{16}$$

In this formulation, $\mathrm{m_{ij}}$, $\mathrm{k_{ij}}$ and $\mathrm{b_{ijkl}}$ represent the mass matrix, the linear stiffness tensor, and the nonlinear stiffness tensor, respectively. Their analytical expressions are given below:

$$\mathrm{K_{ij}} = \mathrm{E_b I_b}\int_0^{\mathrm{L_1}}\left(\frac{\partial^2 \mathrm{W_i}}{\partial \mathrm{x}^2}\right)\left(\frac{\partial^2 \mathrm{W_j}}{\partial \mathrm{x}^2}\right)\mathrm{dx} + E_c A_c(\sin\theta)^2 W_i\int_0^{L_c} W_j \mathrm{dx} + \sum_{i=1}^{n} K_{T\ Sring}\, W_i\left(x_{T\ Sring}\right)\mathrm{W_j}\left(x_{T\ Sring}\right) + \sum_{i=1}^{n} K_{R\ Sring}\frac{\partial \mathrm{W_i}(x_{R\ Sring})}{\partial \mathrm{x}}\frac{\partial \mathrm{W_j}(x_{R\ Sring})}{\partial \mathrm{x}} \tag{17}$$

$$b_{ijkl} = \frac{\mathrm{E_b S_b}}{4L_b}\int_0^{L_b}\left(\frac{\partial W_i}{\partial x}\right)\left(\frac{\partial W_j}{\partial x}\right)dx\int_0^{L_b}\left(\frac{\partial W_k}{\partial x}\right)\left(\frac{\partial W_l}{\partial x}\right)dx \tag{18}$$

$$m_{ij} = \rho_b S_b \int_0^{L_1} W_i W_j dx \tag{19}$$

By substituting Eqs. (14), (15), and (16) into Eq. (7), and after simplification, the following expression is obtained:

$$2a_i k_{ir} + 3a_i a_j a_k b_{ijkr} - 2\omega^2 a_i m_{ir} = 0 \tag{20}$$

Prior to determining the contribution coefficient aia_iai and the associated natural frequency ω, Eq. (13) is rewritten in a nondimensional form by replacing the dimensional parameters with their corresponding reduced (dimensionless) counterparts.

$$x = Lx^* \quad \text{and} \quad W(x) = HW^*(x^*) \tag{21}$$

In this expression, H denotes the characteristic height of the beam. Assuming that the beams illustrated in Fig. 1 are geometrically identical, the tensor expressions can therefore be written as follows:

$$m_{ij}^* = \int_0^1 W_{1i}^* W_{1j}^* dx^* \tag{22}$$

$$k_{ij}^* = \int_0^1 \left(\frac{\partial^2 W_{1i}^*}{\partial \mathrm{x}^{*2}}\right)\left(\frac{\partial^2 W_{1j}^*}{\partial \mathrm{x}^{*2}}\right) \mathrm{d}x^* + (\sin\theta)^2 W_{1i}^* \int_0^{L_c} W_{1j}^* \mathrm{d}x^* + \sum_{i=1}^{n} K_{T\,Sring}\, W_{1i}^*\left(x_{T\,Sring}\right) W_{1j}^*\left(x_{T\,Sring}\right) + \sum_{i=1}^{n} K_{R\,Sring} \frac{\partial \mathrm{W}_i(x_{R\,Sring})}{\partial x^*} \frac{\partial \mathrm{W}_j(x_{R\,Sring})}{\partial x^*} \tag{23}$$

$$b_{ijkl}^* = \alpha \int_0^1 \left(\frac{\partial W_{1i}^*}{\partial x^*}\right)\left(\frac{\partial W_{1j}^*}{\partial x^*}\right) dx \int_0^1 \left(\frac{\partial W_{1k}^*}{\partial x^*}\right)\left(\frac{\partial W_{1l}^*}{\partial x^*}\right) dx^* \tag{24}$$

By substituting Eqs. (22), (23), and (24) into Eq. (20), the following system of nonlinear algebraic equations is obtained:

$$2a_i^* k_{ir}^* + 3a_i^* a_j^* a_k^* b_{ijkr}^* - 2\omega^{*2} a_i^* m_{ir}^* = 0 \tag{25}$$

The equation was solved using a single-mode reduced modal approach, initially developed by Benamar and Kadiri in [16]. This method focuses exclusively on the dominant vibration mode, assuming its predominance in the nonlinear response, while neglecting the contributions of higher-order modes.

$$\left(\frac{\omega_{nl}^*}{\omega_l^*}\right)^2 = 1 + \frac{3}{2} a_i^2 \frac{B_{iiii}}{K_{ii}} \tag{26}$$

With :

$$\omega_l^* = \frac{K_{ii}}{m_{ii}} \tag{27}$$

NUMERICAL RESULTS AND DISCUSSION

Linear Vibration Analysis

This section first presents the results related to the linear part of the problem, followed by those obtained from the nonlinear analysis. The linear natural frequencies were computed using the material properties reported in[14], considering three beam configurations: clamped–clamped, simply supported–simply supported, and clamped–simply supported. The comparison between the obtained results and those available in previous studies by [17] shows an excellent agreement, thereby confirming the reliability of the adopted methodology.

Table 1 provides a detailed comparison between the natural frequencies obtained in the present study and those reported in previous works, highlighting the high accuracy of the computed results. An excellent agreement is observed, with negligible discrepancies for the first six vibration modes. This consistency confirms the reliability and relevance of the adopted analytical and methodological approaches, in accordance with the reference data available in the scientific literature.

TABLE 1. Comparison of the first six natural frequencies of double cable-stayed beams in SS, CS, and CC cases.

Natural frequency	Present study (SS)	Theoretical value (SS) [15]	ANSYS (SS) [15]	Present study (CC)	Present study (CS)
1st	0,1362	0,1355	0,1360	0,1680	0,1480
2nd	0,2310	0,2307	0,2307	0,3370	0,2770
3rd	0,4354	0,4354	0,4349	0,5940	0,5140
4th	0,7849	0,7848	0,7840	0,9850	0,8810
5th	1,2162	1,2162	1,2147	1,4700	1,3360
6th	1,3428	1,3503	1,3436	2,0440	1,3420
K_{T1}	0	0	0	∞	∞
K_{T2}	0	0	0	∞	0
$K_{\theta 1}$	∞	∞	∞	∞	∞
$K_{\theta 2}$	∞	∞	∞	∞	∞

Nonlinear Vibration Analysis

To validate the proposed variational approach for analyzing the nonlinear vibrations of a beam suspended by two elastic cables located at x=L/3 and x=2L/3 along its total span, a parametric study is carried out by introducing translational and rotational elastic supports at both ends. The translational stiffnesses are assumed to approach infinity ($K_{t1} = K_{t2} = \infty$), whereas the rotational stiffnesses are varied according to $K_{\theta i} = (0, 10, 100)$.

The objective of this section is to investigate the influence of the maximum vibration amplitude W^*_{max} on the dynamic behavior of the beam. This effect is illustrated through the nonlinear mode shape and the corresponding curvature for each value of K_θ. In the context of free vibration analysis, the dimensionless nonlinear frequency ω^*_n is compared to the linear frequency ω^*_lusing the ratio ω^*_n/ω^*_l, expressed as a function of the dimensionless maximum amplitude W^*_{max}.

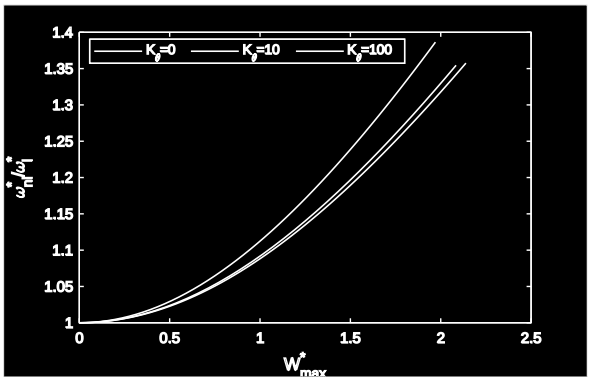

FIGURE 2. Variation of the frequency ω^*_n/ω^*_l as a function of the dimensionless maximum amplitude W^*_{max}, for different values of the rotational stiffness K_θ

Figure 2 highlights the influence of the rotational stiffness of the supports, K_θ, on the nonlinear free vibration response of the beam suspended by elastic cables. It can be observed that the frequency ratio ω^*_n/ω^*_lincreases gradually with the dimensionless maximum amplitude W^*_{max}, indicating a hardening-type behavior that is characteristic of geometric nonlinear effects.

- For $K_{\theta 1} = K_{\theta 2} = 0$ (supports free in rotation), the curve exhibits the steepest slope, indicating a pronounced nonlinearity where the frequency increases rapidly with amplitude.
- For $K_{\theta 1} = K_{\theta 2} = 10$, the curve lies slightly below the previous one, showing that a moderate rotational stiffness slightly reduces the hardening effect.

- For $K_{\theta 1} = K_{\theta 2} = 100$, the response becomes stiffer in rotation; the curve flattens, and the sensitivity of the frequency to the amplitude decreases significantly.

Thus, as K_θ increases, the beam response tends toward a quasi-linear behavior, with the geometric nonlinearity becoming progressively less significant.

To investigate the influence of the rotational stiffness at the beam ends on its nonlinear dynamic behavior, Figure 3 illustrates the distribution of the curvature $\frac{d^2W(x)}{dx^2}$ corresponding to the first vibration mode. The results are presented for three boundary conditions, $K_{\theta 1} = K_{\theta 2} = 0, 10\ and\ 100$, and for two values of the dimensionless vibration amplitude W^*_{max}. This comparison reveals the combined effects of rotational stiffness and geometric nonlinearity on the modal shape and the curvature concentration near the beam supports.

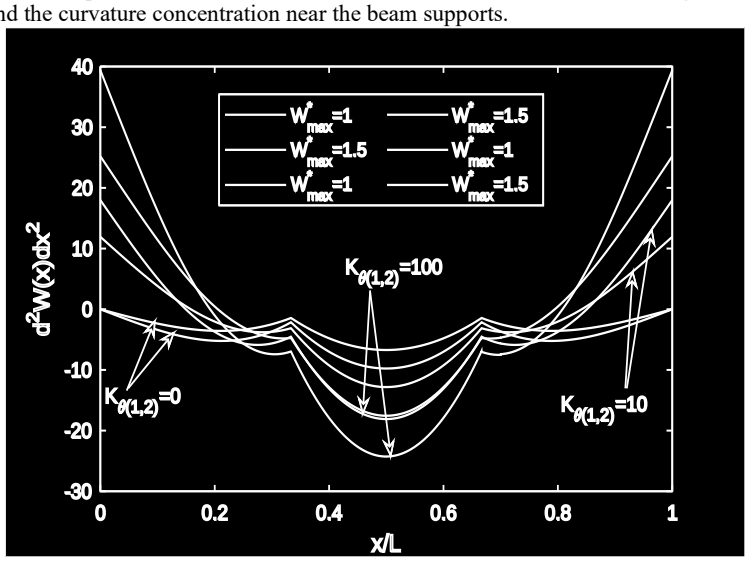

FIGURE 3. Curvatures of a cable-stayed beam near the first mode for $K_{\theta 1} = K_{\theta 2} \in \{0, 10, 100\}$ and two vibration amplitudes $W^*_{max} \in \{1, 1.5\}$

When transitioning from $K_{\theta 1} = K_{\theta 2} = 0$ (free supports) to 10 and then to 100, the following trends are observed:

- A noticeable increase in the positive curvature peaks near the beam ends, accompanied by an enhancement of the negative curvature around the mid-span region.
- A shift of the inflection points toward the supports, indicating a gradual transition from an almost simply supported behavior to a quasi-clamped one.
- A modal shape that becomes stiffer near the ends (formation of pronounced boundary layers), while maintaining symmetry with respect to the mid-span.

An increase in the dimensionless maximum amplitude W^*_{max} intensifies the geometric nonlinearity, as evidenced by the nonlinear deviations observed between $W^*_{max} = 1\ and\ 1{,}5$, particularly for higher values of K_θ.

CONCLUSION

The present study developed a single-mode analytical model for analyzing the geometrically nonlinear free vibrations of a cable-supported beam with elastic end supports. Based on Hamilton's principle and the Euler–Bernoulli beam theory, the proposed method—solved using the Newton–Raphson iterative algorithm—accurately predicts the evolution of natural frequencies and mode shapes as a function of the vibration amplitude. The results highlight a hardening-type spring behavior and emphasize the significant influence of the rotational stiffness of the supports on the dynamic response. The proposed model proves to be both accurate and computationally efficient, providing a solid framework for the extended analysis of beam–cable systems under more complex boundary and loading conditions.

REFERENCES

1. M. Berjal, A. Adri, O. Outassafte, I. E. Hantati, Y. E. Khouddar, M. Rjilatte, and R. Benamar, Parametric Analysis Studies of the Vibrations of a Multi-Cable-Stayed Beam Resting on Elastic Support, SSRG-IJCE 11 1–19 (2024).
2. M. Rjilatte, A. Adri, O. Outassafte, I. E. Hantati, Y. E. Khouddar, M. Berjal, and R. Benamar, In-Plane Vibration Analysis of a Multi-Cable-Stayed Beam Carrying Concentrated Masses and the Impact of Thermal Effects, SSRG-IJCE 11 107–119 (2024).
3. H. Kang, Y. Cai, Y. Cong, X. Su, and G. Yan, revealing energy transfer between deck and cables in cable-stayed bridges through resonancne analysis with coupling effect of adjacent cables considered, (2022).
4. J. Peng, M. Xiang, L. Wang, X. Xie, H. Sun, and J. Yu, Nonlinear primary resonance in vibration control of cable-stayed beam with time delay feedback, Mechanical Systems and Signal Processing 137 106488 (2020).
5. V. Gattulli, and M. Lepidi, Nonlinear interactions in the planar dynamics of cable-stayed beam, International Journal of Solids and Structures 40 4729–4748 (2003).
6. L. Azrar, R. Benamar, and R. G. White, semi-analytical approach to the non-linear dynamic response problem of s–s and c–c beams at large vibration amplitudes part i: general theory and application to the single mode approach to free and forced vibration analysis, Journal of Sound and Vibration 224 183–207 (1999).
7. M. El Kadiri, R. Benamar, and R. G. White, Improvement of the semi-analytical method, for determining the geometrically non-linear response of thin straight structures. part i: application to clamped–clamped and simply supported–clamped beams, Journal of Sound and Vibration 249 263–305 (2002).
8. I. El Hantati, O. Outassafte, Y. El Khouddar, M. Belhaou, A. Adri, and R. Benamar, Analysis of the transverse vibration of a multistepped FGM beam resting on a Winkler foundation in a thermal environment and carrying concentrated masses, Results in Engineering 23 102822 (2024).
9. O. Outassafte, A. Adri, Y. E. Khouddar, I. E. Hantati, S. Rifai, and R. Benamar, Crack identification in circular arches through natural frequency variations and the firefly hybrid algorithm, Mechanics of Advanced Materials and Structures 31 5701–5715 (2024).
10. A. Oudra, Y. E. Khouddar, A. Adri, O. Outassafte, I. E. Hantati, H. Isksioui, and H. E. Moussami, Vibration control and analysis of Terfenol-D functional gradient material beams with porosities: Linear and nonlinear perspectives in thermal environments, ZAMM - Journal of Applied Mathematics and Mechanics / Zeitschrift für Angewandte Mathematik und Mechanik 104 e202400236 (2024).
11. I. El Hantati, A. Adri, H. Fakhreddine, S. Rifai, and R. Benamar, Multimode Analysis of Geometrically Nonlinear Transverse Free and Forced Vibrations of Tapered Beams, Shock and Vibration 2022 1–22 (2022).
12. Y. El Khouddar, A. Adri, O. Outassafte, S. Rifai, and R. Benamer, Non-linear forced vibration analysis of piezoelectric functionally graded beams in thermal environment., International Journal of Engineering 34 2387–2397 (2021).
13. V. Gattulli, M. Morandini, and A. Paolone, A parametric analytical model for non-linear dynamics in cable-stayed beam, Earthq Engng Struct Dyn 31 1281–1300 (2002).
14. M. Berjal, A. Adri, O. Outassafte, I. E. Hantati, Y. E. Khouddar, M. Rjilatte, and R. Benamar, Linear vibration analysis of multi-cable-stayed beams resting on multiple elastic supports, In, AIP Publishing, Varna, Bulgaria, (2024), 020012.
15. 丛云跃, 康厚军, 郭铁丁, 苏潇阳, and 金怡新, CFRP索斜拉桥面内自由振动的多索梁模型及模态分析, 动力学与控制学报 15 494–504 (2017).
16. F. T. K. Au, D. Y. Zheng, and Y. K. Cheung, Vibration and stability of non-uniform beams with abrupt changes of cross-section by using C1 modified beam vibration functions, Applied Mathematical Modelling 23 19–34 (1999).
17. M. Rjilatte, A. Adri, O. Outassafte, I. E. Hantati, Y. E. Khouddar, M. Berjal, and R. Benamar, Dynamic behavior analysis of a multi-cable-stayed beam carrying concentrated masses, In, AIP Publishing, Varna, Bulgaria, (2024), 020009.